

Thermoelectric effect in a ring with a Josephson junction

R. M. Arutyunyan, G. F. Zharkov, G. Yu. Logvenov, V. V. Ryazanov, and V. V. Shmidt

Institute of Solid State Physics, Academy of Sciences of the USSR; Energiya Scientific-Manufacturing Alliance; P. N. Lebedev Physics Institute, Academy of Sciences of the USSR, Moscow

(Submitted 6 January 1984)

Zh. Eksp. Teor. Fiz. **87**, 596–604 (August 1984)

Experiments reveal the induction of magnetic flux in a bimetallic superconducting system—a ring closing the circuit for an SNS Josephson junction—when there is a heat flux through the junction. The behavior of the system is simulated numerically on the basis of a theory derived for the uniform introduction of an electric current into a distributed SNS junction whose circuit is closed by a superconducting ring.

INTRODUCTION

Thermoelectric phenomena in superconductors are the subject of a lively discussion in the literature these days.^{1,2} Among the superconducting systems which have been involved in attempts to observe effects of this sort we can distinguish two large groups: the various bimetallic or inhomogeneous superconductors (Refs. 1 and 2; see also Ref. 3) and the weakly linked superconductors.^{4–6} Some interesting magnetothermoelectric and magnetoelectric phenomena are observed in distributed SNS Josephson junctions.^{6–8} The specific behavior of these systems stems from the dynamics of the Josephson vortices which arise and propagate in the junction.

In this paper we examine how a heat flux or electric current through a distributed Josephson junction would affect the behavior of a massive superconducting ring which closes the circuit for this junction. We report theoretical and experimental research on the behavior of the magnetic flux produced in a ring with a weak link in response to a heat flux. It is our hope that further research in this field will cast light on the physical mechanisms for thermoelectric phenomena in bimetallic superconducting rings and SNS Josephson junctions.

THEORY

We consider a weakly linked distributed junction of length L whose circuit is closed by a massive superconducting ring with an inductance \mathcal{L} (Fig. 1). We assume that the

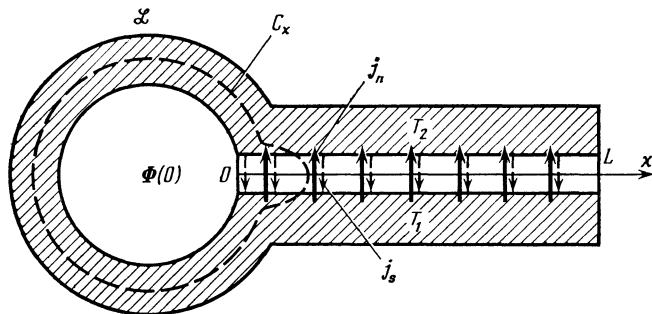


FIG. 1. Schematic diagram of a system with a distributed Josephson junction for which the circuit is closed by a massive superconducting ring (a single-contact interferometer). \mathcal{L} —Inductance of the ring; L —length of the junction. The normal current in the junction is set by the temperature difference $T_2 - T_1$ between the boundary regions of the weak link.

dimension (w) of the junction along the z axis (which runs perpendicular to the plane of Fig. 1) is small—smaller than the Josephson penetration depth λ_J . The current distribution near the weak link can thus be assumed to depend on only the coordinate along the junction, x , in precisely the same manner as in the case in which the junction and the ring have infinite dimensions along z . We accordingly restrict the analysis to the solution of the one-dimensional problem. We assume that there is no external magnetic field. This assumption simplifies the calculations but is not crucial, since the incorporation of a static external field and a “frozen-in” magnetic flux in the ring would actually do nothing more than shift the origin, having no substantial effect on the shape of the curves [see Eq. (13) below]. For a qualitative discussion of the experimental data obtained in the presence of a “remanent” external magnetic field we will accordingly use equations which ignore the initial frozen-in flux.

We now assume that a temperature difference $T_2 - T_1$ is maintained between the boundaries of the weak-link region in the junction. A normal-excitation current $j_n = b(T_2 - T_1)$, where b is the thermoelectric coefficient of the weak link, flows through the junction (an SNS junction, for example). In addition to the current j_n , a superconducting current of Cooper pairs j_s flows through the junction; if the circuit of the junction is open, this current cancels the normal current^{9,6}: $j = j_n + j_s = 0$. If the junction is connected in a superconducting ring, the currents will not cancel exactly, and some resultant thermoelectric current I , for which the ring closes the circuit, will flow through the junction. A magnetic flux $\Phi(0)$ accordingly arises in the ring.

To find the flux $\Phi(0)$ we use a Ferrell-Prange equation

$$d^2\varphi(x)/dx^2 - \sin\varphi(x) + j_0 = 0, \quad (1)$$

which describes the behavior of a distributed Josephson junction in the steady state and for a homogeneous inflow of the external electric current into the junction. The applicability of this equation in the case of a heat flux was discussed in Ref. 7. The units in Eq. (1) are dimensionless, as usual. Here $j_0 = j_n/j_c$, where j_n is the normal thermoelectric current density through the junction, j_c is the critical current density of the junction, adopted as a unit, and $j_s(x) = \sin\varphi(x)$ is the superconducting current density. Distance along the junction is expressed in units of the Josephson penetration depth $\lambda_J = (\Phi_0/2\pi \mathcal{L} j_c)^{1/2}$. The magnetic field H is expressed in units of $H_J = \Phi_0/2\pi\lambda_J A$, where $\Phi_0 = h/2e$ is the quan-

tum of magnetic flux, $\Lambda = 2\lambda_L = d$ is the thickness of the layer in the junction in which there is effectively a magnetic field,¹⁾ λ_L is the London penetration depth, and d is the thickness of the weak-link region. The inductance per square of the distributed junction can be written as $\mathcal{L}_\square = \mu_0\Lambda$, where $\mu_0 = 4 \cdot 10^{-7}$ H·m, and where we are ignoring edge effects.

In the absence of any heat flux, the phase difference across the weak link is given by the following expression¹⁰ for a single-contact interferometer with a distributed junction: $\varphi(x) = 2\pi\Phi(x)/\Phi_0$, $\Phi(x)$ is the total magnetic flux linked by the contour C_x (Fig. 1) which encloses the aperture and is in the interior of the superconductor everywhere except at the junction. At the junction, it passes through the point x . It is easy to show that if there is a heat flux through the ring, which gives rise to countercurrents $j_s = -j_n$ in the mass of the ring,¹ the expression for the phase difference is modified:

$$\varphi(x) = 2\pi[\Phi(x) + \Phi_T]/\Phi_0$$

(Φ_T is the magnetic flux produced by the thermoelectric current due to the temperature gradient in the massive ring). The ratio Φ_T/Φ_0 , however, is very small. According to estimates in Ref. 1, for temperatures near T_c it is $\Phi_T/\Phi_0 \lesssim 10^{-2}$. In the experiments which we will be discussing below, the temperature T of the superconducting ring was well below T_c , so that this estimate of Φ_T/Φ_0 , made for $(T_c - T)/T_c \sim 10^{-2}$, is in fact a flagrant overestimate. Accordingly, again in the case under consideration here the phase difference $\varphi(x)$ is the same as the total (normalized) magnetic flux in the closed contour C_x .

To find solutions of Eq. (1) we must specify some appropriate boundary conditions. A boundary condition at $x = 0$ can be found from the following considerations. We denote by $I(x)$ the current flowing along the outer electrodes of the distributed junction at point x . The derivative $d\varphi/dx$ at this point is

$$\frac{d\varphi}{dx} = \frac{2\pi}{\Phi_0} \mathcal{L}_\square \frac{\lambda_J}{w} I(x), \quad (2)$$

where w is the dimension of the distributed junction along the z axis. On the other hand, the phase difference at $x = 0$ is $\varphi_0 = 2\pi\Phi(0)/\Phi_0$, where $\Phi(0) = \mathcal{L}I(0)$. Substituting in $I(0)$ from (2), we finally find

$$\left. \frac{d\varphi}{dx} \right|_{x=0} = \frac{\varphi_0}{\sigma}, \quad \sigma = \frac{\mathcal{L}}{\mu_0\Lambda} \frac{w}{\lambda_J}; \quad (3)$$

σ has the meaning of the relative inductance of the ring (or the relative area of the aperture of the ring if the ring dimension along the z axis, w , is large enough).²⁾ This quantity depends on the temperature since λ_J varies in proportion to $j_c^{-1/2}$ as the temperature is varied (the temperature dependence is particularly strong in the case of an SNS junction at temperatures well below T_c).

The other boundary condition is

$$\left. \frac{d\varphi}{dx} \right|_{x=L} = 0, \quad (4)$$

which means that there is no external magnetic field at the point $x = L$ (or means that there is no current entering the edge of the junction).

Equation (1) has the integral

$$\frac{1}{2} \left(\frac{d\varphi}{dx} \right)^2 + \cos \varphi + j_0 \varphi = C, \quad (5)$$

where the arbitrary constant C is determined by condition (4): $C = \cos \varphi_L + j_0 \varphi_L$ [here $\varphi_L \equiv \varphi(L)$]. Condition (3) allows us to put (5) in the form

$$\cos \varphi_L - \cos \varphi_0 + j_0(\varphi_L - \varphi_0) = \varphi_0^2/2\sigma^2, \quad (6)$$

from which we can find φ_L as a function of φ_0 and j_0 . Using (5), we can write the solution of Eq. (1) in the implicit form

$$\int_{\varphi_0}^{\varphi(x)} \frac{dy}{[\cos \varphi_L - \cos y + j_0(\varphi_L - y)]^{1/2}} = x\sqrt{2}. \quad (7)$$

In the case $j_0 = 0$ the integral in (7) reduces to an elliptic integral, and $\varphi(x)$ can be expressed in term of the amplitude Jacobi function. At $j_0 \neq 0$ the function $\varphi(x)$ is more complicated; no analytic theory has been derived for such functions.

Since we were not able to find an analytic expression for the solution of nonlinear equation (1), we found one numerically, using boundary conditions (3) and (4). From the solution we calculated the possible values of the normalized flux in the ring, $\varphi_0 = 2\pi\Phi(0)/\Phi_0$, as a function of j_0 . Figure 2 shows the results of these calculations for several values of L and σ .

We can also find some analytic results which apply to limiting cases of this problem. For example, setting $x = L$ in (7), we find the exact relation

$$\int_{\varphi_0}^{\varphi_L} \frac{dy}{[\cos \varphi_L - \cos y + j_0(\varphi_L - y)]^{1/2}} = L\sqrt{2}, \quad (8)$$

which, along with (6), determines φ_0 as a function of j_0 , L , and σ . Under conditions (6) and (8), condition (4) is satisfied automatically. In the limit $j_0 \gg 1$ Eqs. (6) and (8) can be solved

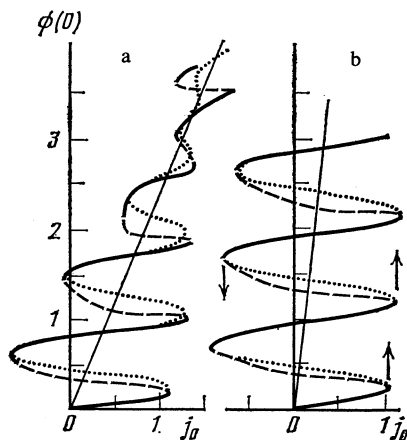


FIG. 2. The reduced magnetic flux in the ring, $\phi(0) = \Phi(0)/\Phi_0$, versus the reduced normal current density in the junction, $j_0 = j_n/j_c$, for several values of the parameters L and σ . a) $L = 3$, $\sigma = 5$; b) $L = 3$, $\sigma = 20$. Solid curves—results of numerical calculations from Eqs. (1), (3), and (4) for stable states; dashed curves—the same, but for unstable states (cf Ref. 10); dotted curves—asymptotic expression (10); arrows—jumps from one branch to another during which the number of flux quanta in the ring changes.

for arbitrary L and σ . Ignoring the terms with the cosines in (6) and (8), we find, respectively,

$$j_0(\varphi_L - \varphi_0) = \frac{\varphi_0^2}{2\sigma^2}, \quad \frac{2(\varphi_L - \varphi_0)^{1/2}}{j_0^{1/2}} = L\sqrt{2},$$

from which in turn we find, in the leading approximation,

$$\varphi_0 = \sigma L j_0, \quad \varphi_L = j_0 L (\sigma + 1/2L), \quad \varphi_L - \varphi_0 = \varphi_0 L / 2\sigma. \quad (9)$$

Rewriting exact relation (6) in the form

$$j_0 = \frac{\varphi_0^2}{2\sigma^2(\varphi_L - \varphi_0)} - \frac{\cos \varphi_L - \cos \varphi_0}{\varphi_L - \varphi_0}$$

and again substituting in the values in (9), we find

$$j_0 = \frac{\varphi_0}{\sigma L} + \sin \left[\varphi_0 \left(1 + \frac{L}{4\sigma} \right) \right] \frac{\sin(L\varphi_0/4\sigma)}{L\varphi_0/4\sigma},$$

$$\varphi_0 = 2\pi \frac{\Phi(0)}{\Phi_0}. \quad (10)$$

Equation (10) determines the functional dependence $j_0(\varphi_0)$ [and also the inverse transcendental function $\varphi_0(j_0)$] at large values of φ_0 (or of j_0). The procedure by which we have derived (10) here cannot be termed rigorous since small terms on the order of $(\cos \varphi_L - \cos \varphi_0)/(\varphi_L - \varphi_0)$ have not been taken into account systematically. Nevertheless, a comparison of the results of the numerical calculations with asymptotic expression (10) (see the dotted lines in Fig. 2) shows that this expression gives a good description of the results of the exact calculations for essentially all values of the parameters. Expression (10) should therefore be regarded as a semiempirical expression which gives a good analytic description of the results of the exact numerical calculation.

When small terms on the order of $(\cos \varphi_L - \cos \varphi_0)/(\varphi_L - \varphi_0)$ are taken into account correctly, we find the following asymptotic formula for $j_0 \gg 1$, but unfortunately this formula gives us the functional dependence of φ_0 on j_0 only implicitly:

$$\sigma^{-1}\varphi_0 = j_0 L + (\pi/2j_0)^{1/2} \sin(\varphi_0 + j_0 L^2/2 - \pi/4). \quad (11)$$

For comparison we also give the asymptotic ($H_L \gg 1$) formula derived in Ref. 10 to describe the penetration of an external magnetic field H_L into a ring interferometer of the type under consideration here. It must be kept in mind that $d\varphi/dx|_{x=L}$ may either be determined by an applied external field H_L or specified by an electric current (I_e) flowing into the edge of the junction from an external source. We write this relation in a form similar to (10):

$$j_e = \frac{\varphi_0}{L\sigma} + \sin \left[\varphi_0 \left(1 + \frac{L}{2\sigma} \right) \right] \frac{\sin(L\varphi_0/2\sigma)}{L\varphi_0/2\sigma},$$

$$\varphi_0 = 2\pi \frac{\Phi(0)}{\Phi_0} \quad (12)$$

($j_e = I_e/L$). Expressions (10) and (12) reveal beats in the magnitude of the hysteresis on the curves of $\varphi_0(j_0)$ (Figs. 2a and 6b) and $\varphi_0(j_e)$ (see Fig. 8a in Ref. 10). The period of these beats in case (10) is twice that in case (12). These beats stem from the effect of the magnetic field on the characteristics of the junction. This effect is described by the factor $\sin(\pi\Phi'/\Phi_0)/(\pi\Phi'/\Phi_0)$ in case (12), in which a current is introduced into the junction from the edge, and by the factor $\sin(\pi\Phi'/$

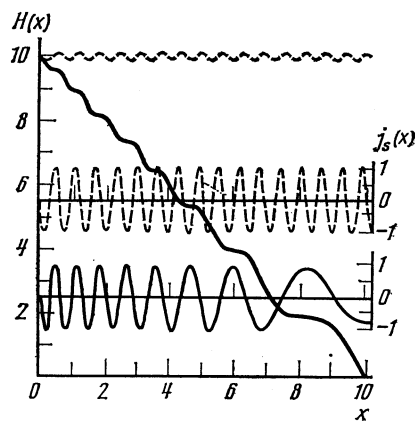


FIG. 3. Distributions of the magnetic field, $H(x)$, and of the superconducting current, $j_s(x)$, in the Josephson junction of an interferometer (Fig. 1) according to calculations from Eq. (1) for $j_0 = 1$, $L = 10$, and $\sigma = 40$ (solid curves). The dashed curves show the same results for $j_0 = 0$, but in the case in which a current I_e corresponding to a reduced external magnetic field $H_e \approx 10$ is introduced into the junction from its edge.

$2\Phi_0)/(\pi\Phi'/2\Phi_0)$ in case (10), in which an external current (or heat flux) is introduced into the junction uniformly. Here $\Phi' = H(0)\Lambda L$, where $H(0)$ is the field which penetrates into the ring, and ΛL is the cross-sectional area of the junction. In the case of an isolated distributed junction (one for which the circuit is not closed by a ring) the effect of an external magnetic field H_e on the critical current is known to be determined by a similar factor, $\sin(\pi\Phi_e/\Phi_0)/(\pi\Phi_e/\Phi_0)$, where $\Phi_e = H_e \Lambda L$ ($L \ll \lambda_J$).

The results of the numerical calculations tell us about the nature of the magnetic structure, i.e., about the distribution and dimensions of the Josephson eddies in the junction. When an electric current is introduced into the junction from its edge (or, equivalently, if there is an external magnetic field), a uniformly distributed chain of eddies of identical size arises in the junction (see Ref. 10 and the dashed curves in Fig. 3). A pressure is exerted on this chain at the $x = L$ edge by the current introduced into this edge from the external source; this pressure is balanced by the effect of the current which flows in the ring and which is linked with the flux $\Phi(0)$. An increase in the density of eddies in the chain corresponds to the presence of these beats on the curves. When a current (or heat flux) enters the junction uniformly, the effect of the current is distributed over the entire junction, so that the eddies which lie relatively close to the $x = L$ edge sense a lower resultant pressure than that experienced by the vortices near the $x = 0$ edge. Consequently, the dimensions of the eddies in the chain are not identical along the junction; they decrease with distance from the $x = L$ edge (solid curves in Fig. 3).

Finally, we give the asymptotic formula for the penetration of a magnetic field into the ring of this interferometer when there is a current j_0 in the system, and an external magnetic field H_L is applied:

$$j_0 L + H_L = H(0) + \sin \left[\frac{H(0) + H_L}{4} L + \sigma H(0) \right] \times \frac{\sin[(H(0) + H_L)L/4]}{(H(0) + H_L)/4}. \quad (13)$$

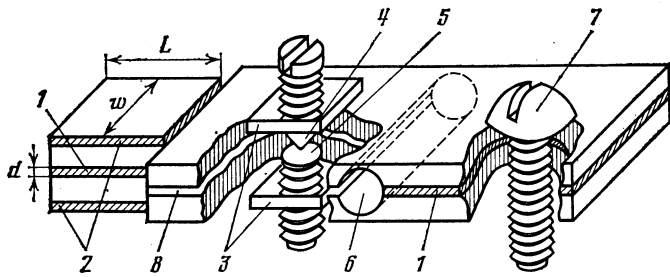


FIG. 4. Construction of the interferometer used in the experiments. 1—Copper interlayer of the Ta-Cu-Ta sandwich; 2—outer copper plating of the SNS junction, used for soldering the heater and the cold finger; 3—nuts holding the screws of the point contact; 4, 5—blunt and sharp screws of the point contact; 6—cylindrical cavity with a cross-sectional area of 0.01 cm^2 (the ring of the interferometer under study and of the rf SQUID); 7—massive superconducting short-circuiting device; 8—gap.

Here $H(0) = \varphi_0/\sigma$, and we are assuming $H(0) \gg 1$. If $H_L = 0$, (13) reduces to (10).

In the case $j_0 = 0$, we can set $H(0) \approx H_L$ in the correction term with the sines in (13) [this approximation is valid at $H(0) \gg 1$]; we find an expression equivalent to (12). It is simple to show that the functional dependence $\varphi_0(j_0)$ described by (13) is qualitatively similar to (10) (Fig. 2) and corresponds to a simple shift of the curves in Fig. 2 along the ordinate axis.

The theory derived above therefore describes several characteristic effects in a single-contact interferometer with a distributed junction: the appearance of a magnetic field in the ring of the interferometer when a temperature gradient is imposed across the junction; jumps in the magnetic flux in the ring associated with the transition of the system from one possible state to another; hysteresis effects associated with these jumps; and beats on the $\Phi(j_0)$ curve. All of these effects have been observed in the experiments which we carried out.

EXPERIMENT

The distributed Josephson junctions used in these experiments were massive Ta-Cu-Ta SNS sandwiches fabricated by joint hot rolling in vacuum.¹¹ The advantages of SNS sandwiches over Josephson junctions of other types for observing thermoelectric phenomena was discussed in Ref. 6. One of the interferometer designs used is shown in Fig. 4. The junction is rectangular. Its length L is varied from 0.3 to 2 cm; the dimension w is 0.3 cm. The thickness of the normal interlayer, d ($\approx \lambda$), is 7, 9, and $13 \mu\text{m}$ in different junctions. The temperature of the superconducting transition (T_c) of the tantalum plates of the junction is 4.37 K. The magnetic flux (Φ) which appears in the superconducting ring (denoted earlier, in dimensionless units, as φ_0) is measured with an rf SQUID.¹² The sensitivity of this SQUID in terms of the flux through its sensitive aperture is no greater than $10^{-3} \Phi_0$.

From (10) and (12) it is a simple matter to find, with reference to the curves of Φ versus the total current injected into the junction, I , that the ratio of the width of the $\Phi(I)$ hysteresis loop along the I axis (Fig. 5a) to the length of the step along the same axis is determined by the ratio $2\pi \mathcal{L} I_c / \Phi_0$. In dimensionless units this quantity is given by the product σL . Here I_c is the critical current in an isolated junction without a field. Consequently, to improve the experimental resolution of the structure of the jumps in the flux it was necessary to reduce the induction of the superconducting ring; this point presented difficulties for the SQUID measurements of the flux Φ . Figure 4 shows the integrated system of the sample (the superconducting ring with a junction)

and the measurement instrument (the rf SQUID). In one common sandwich plate a slice has been removed by electric-arc cutting everywhere in the plane of the normal interlayer except at the junction (with dimensions of $3 \times 3 \text{ mm}$). A cavity 6 (the superconducting ring) was drilled in the center of the plate; the axis of this cavity lies in the plane of the slice removed. On the side opposite the junction the gap is bridged by a massive superconducting short-circuiting device 7. Between the cavity and the junction the gap is bridged by a point superconducting contact (4, 5). The point contact, the cavity, and the massive bridge form the circuit which is used as an rf SQUID. The junction, the cavity, and the bridge constitute the system under study. During rf pumping by the SQUID coil (this coil is placed in cavity 6) the point contact is not a superconducting short-circuiting device for the low-frequency signals studied in this system. The magnetic flux to be measured is thus transported almost ideally to the SQUID; furthermore, comparatively low inductances \mathcal{L} ($\sim 10^{-10} \text{ H}$) were achieved for the superconducting cavity. By varying the temperature of the helium bath it is a simple matter to vary the parameters of the theory, σ and L , through an exponential variation of the critical current density (j_c) in a junction with a temperature T . For example, in one of the samples at $T = 3.5 \text{ K}$ ($I_c \approx 40 \mu\text{A}$) the values of σ and L were 40 and 1, respectively, and increased significantly with a further decrease in the temperature.

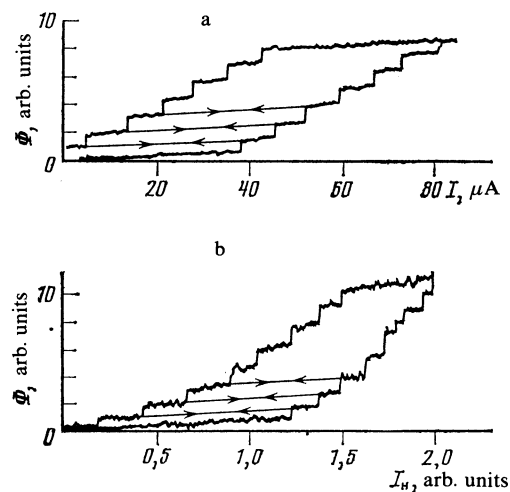


FIG. 5. Response of the interferometer (a) to an electric current introduced into the edge of the junction from an external source and (b) to a heat flux from a heater through whose bifilar winding a current I_H is flowing. These experiments were carried out $T = 4.04 \text{ K}$, $L = 1.1$, and $\sigma = 42$.

To ensure that the rf and low-frequency signals in this system with the rf SQUID did not substantially affect the behavior of the system under study, we carried out some experiments in a simpler but less sensitive system. A superconducting cylinder of a thin niobium foil was connected to the SNS junction described above and inductively coupled with an ordinary Zimmermann rf SQUID. Comparison of the results obtained by the two different measurement methods revealed no substantial differences in the behavior of the curves in the two systems.

The experiments were carried out in a magnetically shielded cryostat. The residual field was estimated to be 10^{-3} G. The temperature was varied by pumping off helium vapor and regulated by a membrane pumping regulator. The experiments involving a heat flux were carried out in a vacuum cup. Heat was applied to the junction from a heater through a bifilar winding through which a current I_H flowed. A cold finger in contact with a liquid-helium bath was attached to the other plate of the SNS sandwich.

In each experiment at the given temperature of the liquid-helium bath, the heat flux and the external electric current (injected at the edge of the junction) were alternately passed across the SNS junction. Since the heat flux is equivalent to a uniform introduction of current into the junction, according to Ref. 7, we were able to experimentally test both expression (10) and expression (12).

Figure 5 shows in detail parts of the $\Phi(I)$ curves (the current was injected into the junction from its edge) and of the $\Phi(I_H)$ curves (again, I_H is the current through the heater; the thermoelectric current which flows uniformly into the junction is proportional to I_H^2). Measurements were taken at $T = 4$ K, $L = 1.1$, and $\sigma = 42$. Figure 6 shows the envelopes of the complex curves with hysteresis and steps for which fragments are shown in detail. The curves are qualitatively identical to the theoretical results calculated from (10) and (12) for the same values of L and σ . A complete quantitative comparison of theory and experiment could not be made because we could not find accurate values of the thermoelectric current in the junction or of the magnetic field in the

working volume. In accordance with (10) and (12), however, the periods of the beats in the magnitude of the hysteresis for the curves in Figs. 6a and 6b [which correspond to the two cases in which the current is introduced into the junction from its edge and in which the current is introduced uniformly (by means of a heat flux)] differ by a factor of about two.

CONCLUSION

In summary, we have experimentally observed the induction of a magnetic flux by the passage of a heat flux through an SNS Josephson junction in a superconducting bimetallic system consisting of the junction and a ring which closes the circuit for it. The penetration of the magnetic flux Φ into the ring with increasing temperature gradient in the junction occurs in discrete steps, and the process is irreversible. The jumps with hysteresis on the curves of Φ versus the heat flux are qualitatively similar to the curves of Φ versus the external magnetic field H_e in a single-contact interferometer.

A numerical simulation of the behavior of this system has been carried out on the basis of a theory derived for the case in which a current is introduced uniformly into a distributed junction for which the circuit is closed by a superconducting ring. Comparison of the results of two types of experiments on this system—with a heat flux passing through the junction and with an electric current introduced into the edge of the junction—confirms the validity of the theoretical model used here. When there is a heat flux through the junction a thermoelectric current arises, distributed uniformly along the junction.

We are indebted to N. S. Stepanov for assistance in fabricating the samples and in carrying out the experiments.

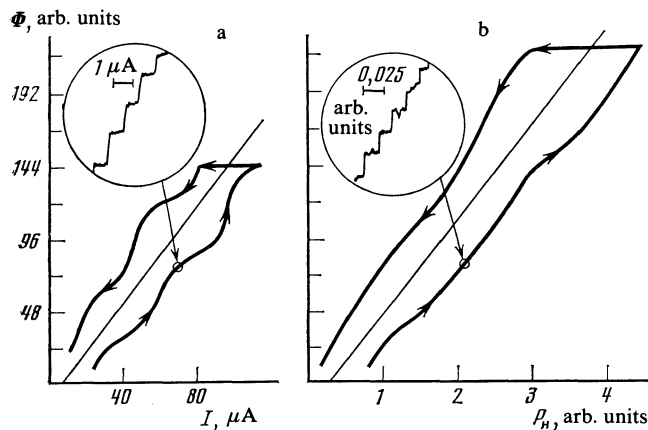


FIG. 6. Envelopes of the interferometer response curves (see the fragments of the curves in the insets). a—Response to an electric current introduced into the edge of the junction from an external source; b—response to a heat flux from a heater with a power $P_H \sim I_H^2$. The experiments were carried out at $T = 3.685$, $L = 3.3$, and $\sigma = 500$.

¹¹In the case of an SNS junction we would have $d \gg \lambda_L$ and thus $A \approx d$. We thus find $H_J \approx \Phi_0 / 2\pi\lambda_J d$.

¹²In the case of an infinitely long sample, φ_0 is related to the magnetic field in the ring, $H(0)$, by $\sigma_0 = \sigma H(0)$ (everything is expressed in terms of dimensionless units).

¹V. L. Ginzburg and G. F. Zharkov, Usp. Fiz. Nauk **125**, 19 (1978) [Sov. Phys. Usp. **21**, 381 (1978)].

²D. J. Van Harlingen, Physica **109-110B** + C, 1710 (1982).

³R. M. Arutyunyan and G. F. Zharkov, Zh. Eksp. Teor. Fiz. **83**, 1115 (1982) [Sov. Phys. JETP **56**, 632 (1982)]; Phys. Lett. **96A**, 480 (1983).

⁴J. Clarke and S. M. Freake, Phys. Rev. Lett. **29**, 588 (1972).

⁵A. G. Aronov and Yu. M. Gal'perin, Pis'ma Zh. Eksp. Teor. Fiz. **19**, 281 (1974) [JETP Lett. **19**, 165 (1974)].

⁶V. V. Ryazanov and V. V. Schmidt, Solid State Commun. **40**, 1055 (1981).

⁷V. V. Schmidt, Pis'ma Zh. Eksp. Teor. Fiz. **33**, 104 (1981) [JETP Lett. **33**, 98 (1981)].

⁸V. V. Ryazanov and V. V. Schmidt, Solid State Commun. **42**, 733 (1982).

⁹V. L. Ginzberg, Zh. Eksp. Teor. Fiz. **14**, 177 (1944).

¹⁰G. F. Zharkov and A. D. Zaikin, Zh. Eksp. Teor. Fiz. **77**, 223 (1979) [Sov. Phys. JETP **50**, 114 (1979)].

¹¹V. V. Ryazanov, V. V. Schmidt, and L. A. Ermolaeva, J. Low Temp. Phys. **45**, 507 (1981).

¹²J. Clarke, in: Weak Superconductivity (Russ. transl.) Mir, Moscow, 1980.

Translated by Dave Parsons